Soft Matter

Accepted Manuscript

ROYAL SOCIETY OF CHEMISTRY

www.rsc.org/softmatter

Journal Name

RSCPublishing

ARTICLE

Light Controlled Friction at a Liquid Crystal Polymer Coating with Switchable Patterning

Cite this: DOI: 10.1039/x0xx00000x

Received 00th January 2012,
Accepted 00th January 2012

DOI: 10.1039/x0xx00000x

www.rsc.org/

Danqing Liu[a], *and Dirk J. Broer*[a,b]* ,

We describe a new methodology that enables dynamical control of motion through modulating friction at coating surfaces by exposing with UV light. The principle is based on reversibly switching the surface topographies of the coating by light. The coating surface transfers from flat in the dark to corrugated in the presence of UV by forming regular ridge-like line gratings. Both the static and the kinetic friction coefficients are investigated in a dynamic manner by switching between the off (flat surface) and the activated (with ridges) state. By dynamically changing the friction, we are able to bring the sample from a static state into motion via UV exposure. When in motion, the friction coefficient can be altered further by modulating the light conditions. E.g. a smooth sliding can transfer into an interlocking state, or vice versa. Moreover, we can dynamically reduce the contact area in the interface and thus lowering friction forces.

Journal Name RSCPublishing

ARTICLE

Introduction

Friction is ubiquitous in nature and our daily activities, ranging from the locomotion of animals to living cell interactions[1,2]. It has been investigated profoundly at both macroscopic and atomic length scales.[3-10] For instance the shape and frequency of well-controlled corrugations were studied at surfaces made from silicone rubber[11] or epoxides[12]. However, modern and advanced technologies are not satisfied with maintaining the friction at a constant value; they require modulation between different levels activated by external triggers[13]. This can be illustrated for example in haptic applications such as touch screens where tactile feedback is provided to the human interface upon a change of the local friction[14,15]. Other fields that benefit from it are, among others, (micro-)robotics, manipulators in medical applications and video games. Friction changes also enable adhesion and release which find potential applications in drug release, motion-manipulated cell culturing and nature inspired adhesives mimicking the so-called gecko effect.[16-18] Most existing systems transform only in one way, e.g. from non-adhering to adhering or vice versa.[19-22] Only a few are able to fulfil the reverse reaction to its original state and achieve repeatability.[23-25] Northen et al described magnetically actuated hairy structures that were rotated either away or towards the countersurface showing reversible adhesion and release[23]. Recently, the Norb's group has demonstrated humidity driven adhesive pads. In all these systems reversibility is established at pre-fabricated surface structures that are permanently present. They provide dynamics by changing shape or orientation. However, those fragile micro- and nanostructures make the surfaces vulnerable to mechanical damages and accumulation of contamination. Moreover, often multiple lithographic fabrication steps are required to produce those delicate patterns which hampers to introduce their application on a large scale or at large surface areas.

To solve these drawbacks, we propose here a design of an advanced coating material that reverses its friction by forming and erasing its surface structures by light. The coating oscillates between a flat surface and a surface with pre-designed 3D micro-patterns by modulating a light source. With recent developments in solid state lighting, light is an attractive trigger medium as it can be integrated in a device for local control or can be used remotely for flood or localized exposure. Therefore light-controlled friction provides a useful tool for many of the mentioned applications.

Without external light source, in the inactivated state, the coating surface is flat, and the friction is direction-independent. In the activated state, when surface patterns are present, the friction becomes directional dependence as set by contact area and potential interlocking of the formed structures. Consequently, depending on the pattern geometry and orientation, the friction will either increase or decrease. We recently reported on the UV induced change in friction at a random fingerprint corrugation[26]. In this communication we report on a new and advanced application towards a direction-dependent switchable friction based on structures with a regular grating pattern that can be turned 'on' and 'off', thereby altering the kinetic friction as well as the static friction.

Results and discussion

Photopolymerized liquid crystal networks (LCN) have demonstrated anisotropic deformation upon a change of their molecular order. These networks are built from stiff rod-like units connected by more flexible polymer main chains. By forming these networks through polymerization of liquid crystal monomers in their oriented state, they exhibit a high degree of molecular order. By design, selecting the appropriate set of liquid crystal monomers and additives, they may respond to various external triggers such as humidity or heat. When the LCN is modified with co-crosslinked azobenzene moieties they will respond to UV or blue light. Under UV illumination, the elongated *trans* azobenzene is converted to the bent *cis* conformation which disturbs the alignment of the surrounding liquid crystal moieties. Consequently, the dimensions change with contraction along the common orientation direction of the molecular units and expansion to the two directions perpendicular to that. Based on this principle, soft actuators are demonstrated, ranging from bending deformation to the more complex origami types of folding.[27-33]

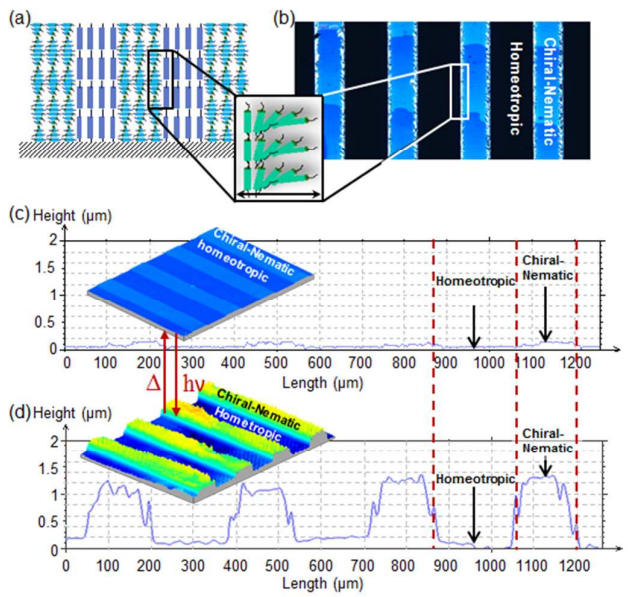

Figure 1. Photo-responsive LC coating. (a) Schematic presentation of LC coating with alternating cholesteric and homeotropic stripes. (b) Polarized optical microscopy images as observed between crossed polarizers. Inset picture elaborates the molecule transition from planar to homeotropic orientation. (c,d) Interferometer measurements. 3D images and their surface profiles of surface topologies at the original state (c) and during illumination with UV light (d).

Recently, we reported on a new effect in shape transformations in terms of switchable surface topographies.[34] In this case, an LCN layer is confined by applying it as a coating on a rigid substrate. Therefore, the deformation can only escape in a dimensional change perpendicular to the coating surface. The coating is made by polymerizing a chiral monomer mixture under a localized electrical field provided by a striped ITO pattern. Still in their monomeric state, the added chirality promotes the formation of helicoidal order where the

average orientation direction of the rod-like molecules describe an helix in the direction perpendicular to the long axes of the molecules. Outside the electrical field the monomers align planar with the helix axes normal to the substrates. Within the areas where the electrical field is present (70 Volts over 5 µm) the monomers follow the field lines and orient with their long axes perpendicular to the substrate while the helix is unwound. This alignment is frozen-in into a crosslinked polymer network by photopolymerization. Consequently, the polymer coating consists of alternating regions of planar helicoidal (long axes of the molecules parallel to the substrate and the helix axes perpendicular to the substrate) and homeotropic (long axes of molecules perpendicular to the substrate) alignment, as illustrated in Figure 1(a). The coating adheres firmly to the glass substrate by means of an adhering polyimide interlayer.

Figure 1(b) shows such coating observed between crossed polarizers. The black stripes are the perpendicularly oriented regions alternated with the blue stripes of the planar helicoidal areas. Outside the polarizing microscope the cholesteric areas have the green appearance because of their reflection at around 500 nm as caused by Braggs related constructive interference at the periodicity of the molecular helix, a well-known phenomenon in chiral-nematic media[35]. From the position of the reflection band we calculated the pitch of the molecular helix to be 312 nm. Allowing for a small deviation related to a different monomer composition this value is in agreement with the prediction based on the helical twisting power of the chiral component that has been published before[36]. Under the microscope, between crossed polarizers the stripes have their blue color appearance because of the anomalous wavelength dependence of the optical rotation around the bandgap. This causes a strong wavelength dependent absorption and transmission by the second polarizer. The stepwise transition from dark blue to light blue corresponds to steps of a π rotation of the helix as caused by a gradual change of the film thickness under confined boundary conditions during preparation prior to polymerization. The lightened up areas between the black and blue stripes are the domain boundaries corresponding to the transition from homeotropic to planar orientation as indicated in the inset picture as shown in Figure 1(a-b). The width of this transition region is determined by the elastic nature of the LC monomers and is around several micrometers.

Under ambient conditions in the absence of UV light, the coating surface is flat (Figure 1(c)) with only minor initial surface reliefs in the order of 70 nm that can be attributed to the ITO imprints during the fabrication process. When exposed with UV light linear corrugations appear (Figure 1(d)) where the cholesteric network tends to expand perpendicular to the surface, while the homeotropic areas tend to contract along the film thickness and expand in the plane of the film. Figure 1(d) shows that the linear protrusions appearing under UV exposure have a height in the order of 1 um, which on a 5 µm thick film corresponds to a strain difference of around 20%. This significant deformation corresponds to the combined action of a density decrease upon conversion from the *trans* to *cis* state of the azobenzene and the opposite photomechanical response of the two areas with different orientation. These results are larger than reported previously for a thermal activated coating with chiral nematic next to isotropic regions[37] and for a mask-wise UV activated homogeneous chiral-nematic LCN coating[38]. By switching off the UV light, the coating immediately relaxes back to the original flat state via thermal processes.

The presence or absence of the ridges are anticipated to affect the friction properties of the surface. Both the static friction and the kinetic friction of the coating are studied accordingly in a dynamic manner, i.e. with and without UV actuation and time resolved during the UV activation/deactivation process.

The static friction coefficient (μ_s) and the influence of ridge orientations are investigated. The static friction coefficient (μ_s) is measured by placing two coatings against each other and tilt them from the horizontal position to a deflection angle β. In horizontal position there is no frictional force, however, as soon as the coatings become slowly tilted the friction force increases and counteracts the component of the gravity force. The static friction force is recorded as soon as the top coating just starts to slide off at an angle β. This angle is known as friction angle. The static friction coefficient is calculated as $\mu_s = \tan\beta = h/L$, where h is the height of the tilted position and L is the length of the projection of the contact area of the coating. The measured static friction coefficient of flat coating is 0.5.

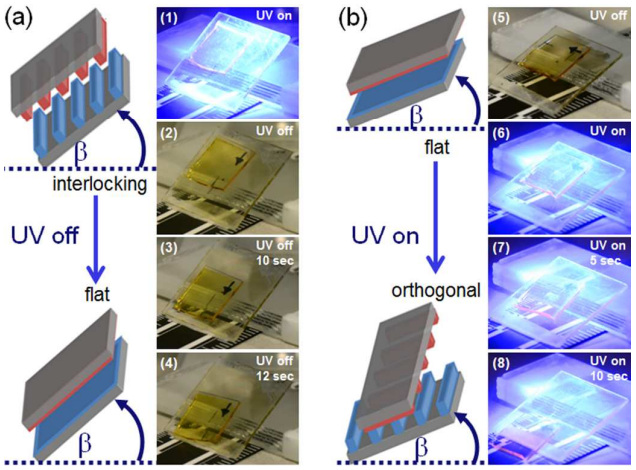

Figure 2. Snap shots of glass plates sliding when the static friction changes (a-d) from an interlocking to a flat state and f(e-f) from a flat to a state with orthogonal alignment. The weight of the top glass plate is 2.47 gram

When the surface is switched from flat to the corrugated state the static friction force is subject to change. Depending on the orientation of the formed gratings, the static friction coefficient increases to 0.7 by interlocking of the ridges (see Figure 2(a)) or decreases to 0.2 when gratings are orthogonally aligned and the contact surface area decreases (Figure 2(b)). Based on this, we provide a novel method of light-controlled motion at the static surfaces by decreasing the friction. Two surfaces are placed on top of each other at a tilt angle that sliding just does not occur. By changing the surface conditions, i.e. switch the static friction coefficient from a high value to a low value by switching the lamp off/ on, sliding of the objects is thus initiated as shown in Figure 2. Figures 2(a)(1-4) demonstrate the motion by stopping UV illumination. The coatings switch from the interlocking state when UV is on to the flat surface by turning off UV light. The glass plate starts sliding within seconds. Figures 2(b)(5-8) illustrate the movement generated by UV irradiation. Under ambient conditions, the coatings are inactive and flat. When exposing with UV light, linear protrusions are formed. If the two coatings

are aligned orthogonally, the static friction force decreased and the top loading starts sliding. Both effects, switching on and switching off the surface relief structures, takes a few seconds to occur explaining the response speed of the sliding sample to the ignition of the UV source.

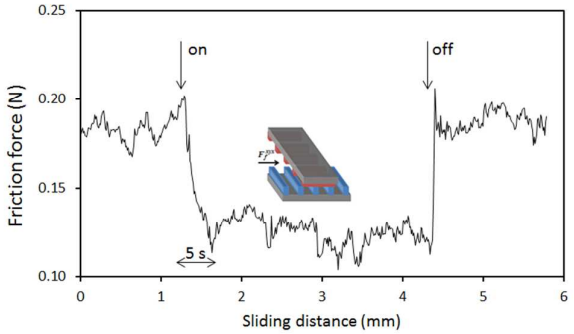

Figure 3. Friction force measured of two sliding glass plates with their LCN coatings facing its other. During the measurement the samples are illuminated (on and off switching of the lamp as indicated) where parallel ridges are being formed with their orientation orthogonal to each other as illustrated by the inset.

When the LCN coated glass plates are in motion, their sliding conditions can be further altered by modulating their surfaces. Figure 3 shows a dynamic experiment where two coated glass plates are sliding against each other at a constant speed under a constant normal load (F_N = 0.5 N) while the LCN coatings at each glass plate are facing each other. Without UV light, the coating is flat and the friction force F_f is of the order of 0.2 N. During sliding the UV lamp is switched on and the exposed surface of the coatings form their ridged structures. In this experiment the axes of the ridges at each side are orthogonal and one can observe a decrease of the sliding force within 5 s after the onset of illumination. After the new sliding force has been stabilized the lamp is switched off again. The friction force responds almost directly by taking its initial higher value again, demonstrating the switchability of the effect. Switching was repeated 25 times with similar results. Microscopic observation of the sample surface however showed some increase of small irregularities because of wear. This has not been part of further investigation at this stage.

This sliding experiment is repeated for three different orientations of the ridges. The results are shown in Figure 4. Initially F_f is again of the order of 0.2 N and independent of the direction. When the UV light is switched on, the linear protrusions are formed and a strong anisotropic frictional behavior is observed. The measured F_f may either increase to 0.3 N, remain unchanged or reduce to 0.1 N depending on the structure geometry and the sliding directions.

When the stripes intersect as shown in Figure 4(a) top, situation F_f^{yyx} (gratings parallel in *y* direction; motion into *x* direction) interlocking occurs. Consequently the friction forces increase. The linear protrusions formed in this specific coating are 1µm in height and 200 µm in width. This relatively low aspect ratio suggests that the structures do not provide the full interlocking which would lead to an unlimited large friction force. Instead, the protrusions hinder the sliding in the x direction and the friction force becomes 1.5 times higher than that of the flat state, as shown in Figure 4(b) red trace. Alternatively, if two coatings slide in the direction parallel to the length of the protrusions (in the y direction, F_f^{yyy}), there are no obstacles and the condition of the sliding is comparable to that of a flat surface. The blue trace in Figure 4(b) indicates that the friction force remains nearly unchanged after switching on the protrusions. On the other hand, if the two sliding coatings have their stripes orthogonally aligned to each other (Figure 4(a) bottom), the contact area between two surfaces is decreased which consequently decreases the friction force (F_f^{xyx}). This corresponds to the green trace in Figure 4(b) where a decrease of F_f by a factor of two is recorded. In all three cases the original friction force of the flat coatings is retrieved in a few seconds by erasing the corrugations through switching off the light illumination.

Figure 4(c) shows a linear relation between friction force (F_f) and normal loading (F_N). In accordance with the first Amontons law of dry friction, the ratio of F_f to F_N is defined as the kinetic friction coefficient, $\mu_k = F_f / F_N$ [39]. From the measurements results we conclude that, under the applied measuring conditions, μ_k is independent of the loading. The kinetic friction coefficient is measured to be 0.4 for a flat coating. It increases to 0.6 when interlocking is activated and drops to 0.2 when the surface contact area is reduced placing the structures of the coating orthogonal to each other.

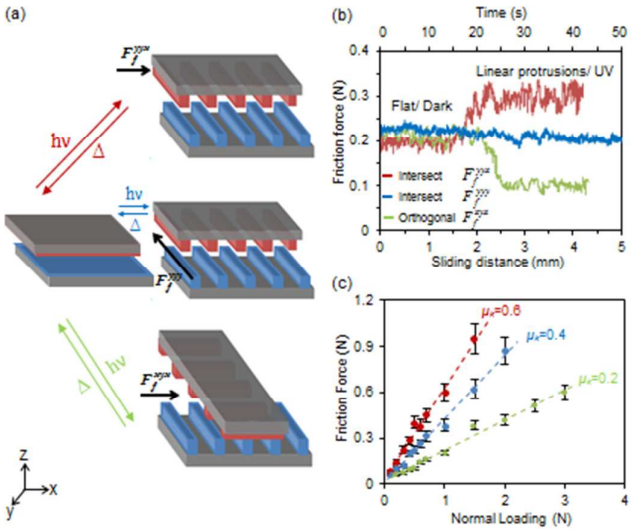

Figure 4. Friction dynamics when linear protrusions are formed and erased. (a) Schematic illustration of the sliding orientation with respect to the orientation of the formed linear protrusions. (b) Dynamic force traces when coatings undergo their transition from flat to corrugated. (c) Friction force as the function of normal loading and the derived friction coefficients.

Friction forces might be affected by adhesion forces between the two sliding surfaces. Extrapolation to zero load in Figure 4(c) reveals a close to zero friction force indicating that the adhesion forces between the two surfaces are also close to zero. The azobenzene molecules are known to increase their dipole moment upon photo-activation.[40] A concern is that the induced polarity could affect the adhesion forces during actuation and thus affect the measurements. Therefore we measured the contact angle with water before and during actuation. In both cases the average contact angle is 72° and does not change within the accuracy of the measurement.

The anisotropy of the friction forces under the formation of the protrusions is further investigated in detail by modifying the angle (θ) between top and bottom coatings, as illustrated in Figure 5. In this experiment, the bottom coating is fixed, while the top coating is kept in a rotated position (Figure 5(a)). The shear force is exerted in the x-direction. The maximum friction coefficient was found when interlocking takes place as the angle between two coatings is $\theta = 0°$ as illustrated in Figure 5(b). A sharp decrease of the friction coefficient was observed when the deflection angle θ is changing from 0° to 20°. This is due to the fact that the interlocking effect rapidly disappears when the two structures are deviating from intersection ($\theta \neq 0°$). From 20° to 90°, the friction force only decreases slightly. In this region, friction force is dominated by the contact area between the sliding coatings which changes slowly till reaches its minimum value at orthogonal alignment (Figure 5(c)). This angular friction coefficient can be described by $F_\theta = \varphi(\theta)F_\perp$. Where F_θ is friction force at angle θ, $F_\perp$ is the friction force for perpendicular ridges and $\theta(\varphi)$ is geometrical factor related to the contact area which can be empirically approximated by $\varphi(\theta) = \sin^{-1/3}(\theta)$. Note that for $\theta = 0°$ F_θ goes to infinity when interlocking occurs. In practice full interlocking does not occur because of a low aspect ratio and the relatively smooth edges at the ridges. Another explanation could be the deformation of the ridges enabling easy sliding. But because of the fact that the coatings are in their glassy state (Tg is around 40 °C) it is considered less likely. Moreover, also inspection of the surface after the experiments did not reveal any changes in the surface due to plastic deformation.

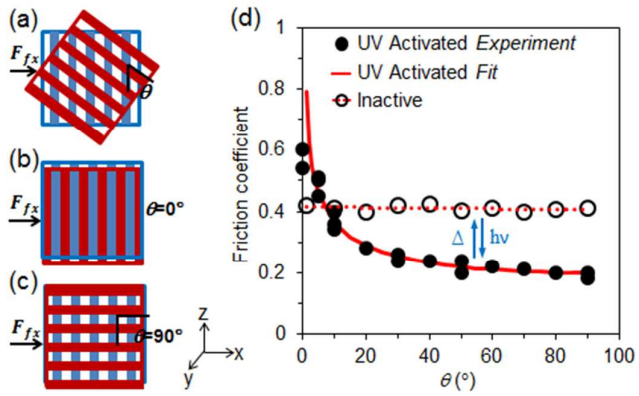

Figure 5. Angular dependence of the friction force. (a) Shows the two coating structures placed on top of each other with angle θ. (b) Interlocking when θ=0°. (c) Two coating structures align orthogonally at θ=90°. (d) Friction coefficient as function of angle between the two coating structures. Red line is the fitted data.

The polymer networks studied are not susceptible to uptake water or other polar liquids and the measurements were done under ambient conditions at room temperature and moderate relative humidity (78±5 %). Nevertheless the question might arise whether the measurements are or could be influenced by the presence of water. Therefore, we repeated our dynamic friction measurements by adding liquid water capillary sucked in between the two responsive layers. When the coatings are flat, water reduces the kinetic friction coefficient from 0.4 to 0.3. Switching on the parallel protrusions, which under the dry conditions provide interlocking, now does not change friction. Apparently water fills the space between the ridges which vanishes interlocking. When the structures are orthogonally aligned, the kinetic friction coefficient is the same for the wet and the dry state. The results are summarized in Table 1. The measured results also suggest that the static and the kinetic friction coefficient are comparable, only slightly higher values are found in the static one. This observation is consistence with that reported for the other materials[41].

Table 1. Measured friction coefficient under different conditions. Comparison of both dynamic and static friction coefficient under dry and wet environments.

Surface	μ_k(dry)	μ_k(wet)	μ_s (dry)	Friction Angle β (°)
Flat	0.45	0.3	0.5	26.5
Interlocking (F_f^{yx})	0.6	0.3	0.7	35
Orthogonal (F_f^{yx})	0.2	0.2	0.2	11.3

Experimental

Materials and Methods

Materials

Scheme 1 shows the mixture used to create smart coatings that can undergo friction changes through exposing to UV light. Monomers **1** to **3** were obtained from Merck UK. Monomer **4** was obtained from BASF. Monomer **5** was custom-synthesized by Syncom (Groningen, the Netherlands). Typically, thin films were fabricated from a mixture containing 20 w% monomer **1**, 39.6 w% monomer **2** and 30 w% monomer **3**, 3.4 w% monomer **4**, 5 w% monomer **5**, 2 w% photoinitiator **6**. The constituents were mixed by dissolving in dichloromethane. DSC results show that the mixture has the chiral-nematic phase in the temperature range between 40°C and 60°C. At higher temperatures the monomer mixture becomes isotropic.

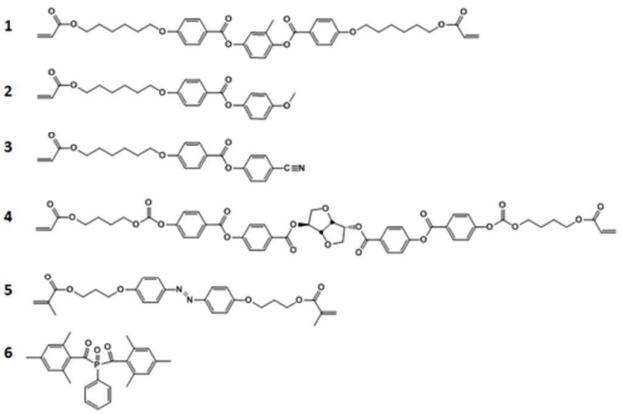

Scheme 1. Materials used for photosensitive dynamic surfaces. Material **1-3** are liquid crystal monomers. **4** is chiral dopant. **5** is azobenzene. **6** is photoinitiator.

Sample preparation

Samples were prepared as published before.[34] Rubbed polyimide AL 1051 (JSR Corporation, Japan) was used to

obtain planar alignment of the liquid crystal monomer mixture. It was spin coated on cleaned ITO glass, followed by baking and unidirectionally rubbing with a polyester cloth.

A stripe patterned coating with alternating areas with planar chiral-nematic order and homeotropic order was made by utilizing a striped ITO electrode pattern at the cover glass plate and a continuous ITO layer at the bottom substrate. The ITO was patterned through spin coating of photoresist, exposure through a mask and etching. To convert the mixture from its planar chiral-nematic orientation to the homeotropic orientation, a voltage of 70V was applied between patterned ITO and continuous ITO glass.

The monomer mixture was capillary filled in between two such treated glass plates and subsequently cured by UV exposure at 45 °C for 30 minutes using a mercury lamp (EXPR Omnicure S2000) equipped with a cut-off filter transmitting light > 400 nm (Newport FSQ-GG400 filter) to prevent isomerization of the azobenzene group during polymerization. The samples were post-baked at 120°C to ensure full cure of the acrylate monomers. Adhesion to the substrate was checked by an adhesive tape test.

Sample characterization

The cholesteric film was checked by polarized microscopy (Leica) enabling discrimination between the planar oriented are and the areas with perpendicular orientation and alignment of the structures when they are brought on top of each other. The surface topography was measured using an interference microscopy (Fogal Nanotech Zoomsurf).

Dynamic Friction Coefficient Measurements

Surface friction is measured in a home-built system[26] by sliding two LCN surfaces against each other with a sliding speed of 0.1 $mm.s^{-1}$. The apparatus is calibrated by sliding different surfaces against each other for which the friction coefficients are known in literature. Examples are glass versus glass and Teflon versus Teflon. These measured values correspond well to the literature values. Alignment of the structures on the two glass plates is achieved by placing the samples against a reference plane after first having check the orientation of the structures by polarizing microscopy. The friction force is measured under various loads, including the load of the top glass plate and is measured under dark conditions as well as under illumination with a mercury lamp (EXPR Omnicure S2000). Occasionally experiments were carried out where the lamp is switched on during the force measurement under dynamic conditions. Similarly, the force was measured while the lamp is switched off.

Static Friction Coefficient Measurements

The static friction coefficient is measured by slowly increasing the tilt angle of two glass plates with respect to the horizontal plane. The glass plates are provided with the same coating with the coating surfaces facing each other. The angle β corresponds to the angle at which the top glass plate just start sliding. The weight of the top glass plate is 2.47 gram.

Conclusions

In conclusion, we have developed a liquid crystal polymer coating that can reversibly change its frictions under illumination. The modulation of the friction is based on a reversible switch between a flat and a pre-designed surface texture. The static friction can be altered by light. It was demonstrated the initiation of the motion starting from a static situation simply by switching on or off the lamp that is illuminating the samples. Moreover, the kinetic friction, when the surfaces are in motion with respect to each other, switches to a lower value by reducing the contact area when the in-situ forming surface structures have only local contact. Conversely, the kinetic friction under motion can be brought to a higher value when the in-situ forming surface structures interlock. Surface friction plays a role in many daily applications, ranging from friction brakes to robotic fingers. Having a tool to manipulate it on the spot will expand on tools design and micro-mechanical applications. An important factor for application is how these coatings will behave under a continuous sliding load. These wear studies are planned for the near future.

Acknowledgements

The results presented are part a research program financed by the Dutch Polymer Institute (DPI), project # 775.

Notes and references

[a] Group Functional Organic Materials & Devices (SFD), Department of Chemical Engineering & Chemistry, Eindhoven University of Technology, Den Dolech 2, 5612 AZ Eindhoven, The Netherlands

[b] Institute for Complex Molecular Systems (ICMS), P.O. Box 513, 5600 MB Eindhoven, The Netherlands

* E-mail: D.Broer@tue.nl

1 M.J. Baum, L.Heepe and S.N. Gorb, Beilstein *Journal of Nanotechnology*, 2014, **5**, 83.

2 M.A. Meyers, P.-Y. Chen, A. Y.-M. Lin, Y. Seki, *Progress in Materials Science*, 2008, **53,** 1.

3 V. V. Tsukruk and V. N. Bliznyuk, *Langmuir,* 1998, **14**, 446.

4 K. Kristiansen, X. Banquy, H. Zeng, E.Charrault, S. Giasson and J. Israelachvili, *Adv. Mater.*, 2012, **24**, 5236.

5 C. Y. Poon and R. S. Sayles, *J. Phys. D: Appl. Phys.*, 1992, **25**, A249.

6 C. Chen, C.Chiang, C.Lai, T.Xie and S.Yang, *Adv.Funct.Mater.*, 2013, **23**, 3813.

7 M. Sedlacek, L.S.Vilhena, B. Podgornik and J.Vizintin, *SV-JME*, 2011, **9**, 674.

8 M. Varenberg and S.N.Gorb, *Adv.Mater.*, 2009, **21**, 483.

9 U. Pettersson and S. Jacobson, *Tribology International,* 2007, **40**, 355.

10 M. Wakuda, Y. Yamauchi, S. Kanzaki and Y. Yasuda, *Wear,* 2003, **254**, 356.

11 B. He, W. Chen and Q.J. Wang, *Tribology Letters*, 2008, **31**, 187.

12 N.B. Tay, M. Minn and S.K. Sinha, , *Tribology Letters*, 2011, **44**, 167.

13 C. Greiner, J.R. Felts, Z. Dai, W.P. King, and R.W. Carpick, *Nanoletters*, 2010, **10**, 4640

14 D.J. Meyer, M. Wiertlewski, M.A. Peshkin and J.E. Colgate, *Haptics Symposium (HAPTICS),* 2014 IEEE (DOI: 10.1109/HAPTICS.2014.6775434)

15 Y. Bar-Cohen, *IJASS*, 2012, **13**, 1.

16 S. Reddy, E. Arzt, A. del Campo, *Adv. Mater.*, 2007, **19**, 3833e.
17 M.T. Northen, C. Greiner, E. Arzt, K. L. Turner, *Adv. Mater.,* 2008, **20**, 3905.
18 L.F.Boesel, C. Greiner, E.Arzt, and A. del Campo, *Adv. Mater.,* 2010, **22**, 2125.
19 Michael Varenberg, and Stanislav N. Gorb, *Adv. Mater.*, 2009, **21**, 483.
20 Shravanthi Reddy, Eduard Arzt and Aránzazu del Campo, *Adv. Mater*., 2007, **19**, 3833.
21 C. Pang, T.-i. Kim, W. G. Bae, D. Kang, S.M. Kim and K.-Y. Suh, *Adv. Mater.*, 2012, **24**, 475.
22 C.-M. Chen , C.-L. Chiang , C.-L. Lai , T. Xie and S. Yang, *Adv. Funct. Mater.*, 2013, **23**, 3813.
23 D.-M. Drotlef , P. Blümler and A. del Campo, *Adv. Mater.*, 2014, **26**, 775.
24 Michael T. Northen, Christian Greiner, Eduard Arzt and Kimberly L. Turner, *Adv. Mater.*, 2008, **20**, 3905.
25 L. Xue, A. Kovalev, K. Dening, A. Eichler-Volf, H. Eickmeier, M. Haase, D. Enke, M. Steinhart and S.N. Gorb, *Nano Lett.*, 2013, **13**, 5541.
26 D.Liu and D.J. Broer, *Angew. Chem. Int. Ed.,* 2014, 53,4542.
27 J.S. Evans, P.J.Ackerman, , D.J.Broer, J.Lagemaat and I.I.Smalyukh, *Phys. Rev. E* 2013, **87**, 032503-1.
28 M.Warner, C. D.Modes and D.Corbett, *Proc. R. Soc. A*, 2010, **466**, 2975.
29 M.Camacho-Lopez, H.Finkelmann, P.Palffy-Muhoray and M.Shelley, *Nat. Mater.*, 2004, **3**, 307.
30 T. J.White, S. V.Serak, N.V.Tabiryan, R. A.Vaia and T.J. Bunning, *J. Mater. Chem.*, 2009, **19**, 1080.
31 C. L.Van Oosten, C.W.M.Bastiaansen and D.J.Broer, *Nat. Mater.*, 2009, **8**, 677.
32 T.Kosa, L.Sukhomlinova, L.Su, B.Taheri, T.J.White and T.J.Bunning, *Nature*, 2012, **485**, 347.
33 Y.Yu, M.Nakano and T. Ikeda, *Nature* 2003, **425**, 145.
34 D. Liu, C. W. M. Bastiaansen, J. M. J. den Toonder and D. J. Broer, *Angew. Chem. Int. Ed.*, 2012, **51**, 892.
35 J.S. Prasad, *Opt. Comm*., 1974, **12**, 389
36 C.Sánchez, F.Verbakel, M.J Escuti, C.W.M Bastiaansen and D.J.Broer, *Adv. Mater.*, 2000, **20**, 74.
37 M. E.Sousa, D. J.Broer, C.W.M. Bastiaansen, L.B.Freund, G. P.Crawford, *Adv. Mater.,* 2006, 18,1842.
38 D. Liu, C. W. M. Bastiaansen, J. M. J. den Toonder and D.J. Broer*, Macromolecules*, 2012, **45**, 8005.
39 R. P. Kusv and J. Q. Whitley, *J. Biomechanics*, 1990, **23**, 913.
40 G. S. Hartley and R. J. W. Le Fèvre, *J. Chem. Soc*., 1939, 531
41 S.Sheppard, B.H.Tongue and T.Anagnos, *Wiley and Sons* 2005 ISBN 0-471-372994, 618.

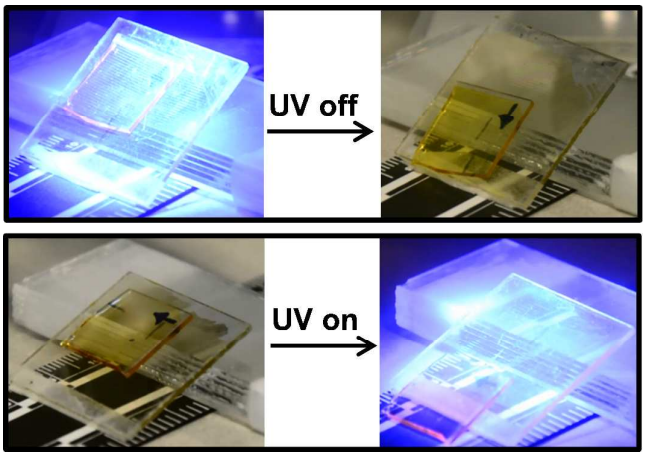

The friction at the coating surfaces can be modulated by light. It is based on reversibly switching the surface topographical patterns of the coating. The samples are brought from a static state into motion just by changing the light conditions.